


11. Gorbatyuk S. M., Zarapin A. Y., Chichenev N. A. Retrofit of vibrating screen of Catoca Mining Company (Angola). *GIAB*. 2018. No. 1. pp. 143–149.
12. Gnezdilov A. A. Implementation of resonant modes of technological vibrational machines. *Bulletin of Altai State Agricultural University*. 2019. No. 1(171). pp. 159–163.
13. Rumiche F., Noriega A., Lean P. et al. Metallurgical failure analysis of a welded drive beam of a vibrating screen. *Engineering Failure Analysis*. 2020. Vol. 118. 104936.
14. Chen Z., Tong X., Li Z. Numerical investigation on the sieving performance of elliptical vibrating screen. *Processes*. 2020. Vol. 8(9). 1151.
15. Blekhman I. I. *Vibration Mechanics and Vibration Rheology (Theory and Applications)*. Moscow : Fizmatlit, 2018. 752 p.
16. Barbosa V. P., Menezes A. L., Gedraite R. et al. Vibration screening: A detailed study using image analysis techniques to characterize the bed behavior in solid–liquid separation. *Minerals Engineering*. 2020. Vol. 154. 106383.
17. Kobelev O., Valeeva L., Gerasimova A. Forging process flow development for plate production. *Solid State Phenomena*. 2021. Vol. 316. pp. 240–245.
18. Lahib M. E., Tekli J., Issa Y. B. Evaluating Fitts' law on vibrating touchscreen to improve visual data accessibility for blind users. *International Journal of Human Computer Studies*. 2018. Vol. 112. pp. 16–27.
19. John Kobbina A., Emmanuel Asuming F., Joe Oteng A. Optimization Algorithms for Solving Combined Economic Emission Dispatch: A Review. *Proceedings of the World Congress on Engineering and Computer Science*. 2019. pp. 210–215.
20. Altshul G. M., Guskov A. M., Panovko G. Ya. Dynamics of a resonant vibrator with an equal-frequency suspension of the working body and an unbalanced vibration exciter. *Obogashchenie Rud*. 2022. No. 1. pp. 51–55.
21. Deniskina T. V. Influence of the shape and angle of the vibrating surface of the working body vibration mill on the quality of the finished product. *GIAB*. 2015. No. 8. pp. 368–372. 

UDC 621.867.2:622.822.24

V. A. MALASHKINA¹, Professor, Doctor of Engineering Sciences, promecology@mail.ru
 A. V. SHAPORTOV¹, Post-graduate student

¹ National University of Science and Technology—NUST MISIS, Moscow, Russia

MODELING HEATING OF FAULTY ROLLER OF BELT CONVEYOR IN THE PRESENCE OF COAL DUST

Introduction

Belts are the common conveying equipment in mines. The high conveying capacity, long haulage and relatively simply maintenance makes this equipment highly popular in underground mining [1].

Alongside with the apparent advantages, the operation of conveyor belts includes complex fire safety control [2, 3]. The main cause of fire in long regions of belt conveyors is the seizure of rollers and the friction between the roller shell and the loaded belt [4, 5]. The friction involves heating of the roller surface and heat emission, which can initiate inflammation of substances having the least burning point, for instance, coal dust [6].

Conveyor lines can be tens kilometers long, and the length of one conveyor can exceed one kilometer. The prompt detection of faults is difficult without special facilities [7, 8] as it is necessary to inspect each roller in the conveyor line, and the number of the rollers may exceed six thousand [9, 10]. The automated fire extinguishment systems are only provided at the power-drive and tension stations of conveyors and are absent along the conveyor flight.

Belt conveyor is a common means of transport in underground mines. At the same time, longwalls equipped with belt conveyors face high fire risk. One of the fire causes on belt conveyors is the seizure of rollers and their friction on the loaded belt in the long flight regions. The modern detectors of fire on belt conveyors fail to ensure ultra early sensing of inflammation. This article describes modeling of heating of a faulty roller in friction with a moving conveyor belt with a layer of coal dust. The modeling has found the rate of heating of the belt conveyor roller up to the temperature of the ultra early fire development with inflammation of coal dust particles, and the degree of effect of the coal dust layer on the fire onset speed. The graphic chart is plotted for the heat balance of a belt conveyor roller in friction-induced heating.

Keywords: coal mine, ore mine, belt conveyor, roller, conveyor belt, exogenous fire, ultra early fire stage, fire initiation signs, heat transfer

DOI: 10.17580/em.2023.01.14

A belt conveyor fire is an exogenous fire controllable using ventilation. Fire begins as inflammation initiated in off-normal mode of a conveyor, and has ultra early, early, developmental, mature and attenuated stages which differ by the ambient temperature. The ultra early and early fire detection enables early localization and elimination of an accident, without work interruption and any severe financial loss. The signs of an early fire can be the CO concentration

in the mine air and the increased temperature in the fire zone. These signs are detected using the point and distributed fire sensors and sending boxes.

Although Russian [11, 12] and foreign [13, 14] researchers investigate fire safety of belt conveyors, the impact of coal dust on the belt–roller shell friction remains beyond the scope of any analysis so far.

This study aims to model fire initiation in a conveyor flight because of the friction between the loaded belt and the shell of a faulty roller with participation of coal dust.

Methods

Modeling of the conveyor belt–coal dust–roller system uses the FEM-based software ANSYS [15, 16].

First, the friction force in the roller–belt and roller–coal dust–belt systems was calculated in unit Transient Structure and, second, the heat effect on the roller was modeled in unit Transient Thermal.

The model region of a conveyor belt is 9.45 m long and has rows of rollers spaced at 1.2 m. The rollers have a diameter of 0.128 m, and the belt has a width of 1 m.

It is assumed in the modeling that the temperature at each point of the roller and belt is initially the same and equals 25 °C, the roller carriage has no lining, and the belt is a uniform material with the uniform characteristics, i.e., the amount of heat emission as heat flows through the multilayered body is disregarded, and each layer has a different heat conduction coefficient. The characteristics selected for the belt and roller materials fit the actual values.

Modeling stage I.

The process uniqueness conditions:

- Dimensions of the roller as per State Standard GOST R 57841–2017: roller shell diameter $d = 0.127$ m, roller shell length $L = 0.380$ m, shell wall thickness $b = 0.004$ m.

- Dimensions of the belt: width, and work and nonwork coat thicknesses—according to State Standard GOST R 57032-2016.

- Belt 2 STS (TG)-1000-4-ER-100/4-5+2-TSO-RB State Standard GOST R represents an orthotropic structure, and the rollers are the elastic solids with the initial parameters of structural steel.

- The belt modeling parameters: density $\rho = 1300$ kg/m³, elasticity moduli along the axes y and z $E_y = E_z = 3.2 \cdot 10^8$ Pa, elasticity modulus along x $E_x = 2.85 \cdot 10^8$ Pa, Poisson's ratio $\nu = 0.4$ and shear moduli along the axes y and z $G_y = G_z = 1.14 \cdot 10^8$ Pa [17]. The FEM cell side is 0.08762 m.

The first-order boundary conditions are described below.

By the Amontons–Coulomb law, the sliding friction force is independent of the contact area between the bodies but depends on the normal reaction force on the bodies and on the properties of materials the bodies are made of [18, 19]:

$$F_{fr} = \mu P, \quad (1)$$

where μ is the friction coefficient; P is the belt pressure, N.

Using (1) and the formula for heat, we obtain:

$$Q_{heat} = \mu P \nu. \quad (2)$$

The heat generated is spent in accordance with the energy preservation law for heating the roller and belt with the coal dust layer, as is given by the heat balance equation [20, 21]:

$$Q_{heat} = Q_r + Q_b, \quad (3)$$

where Q_r and Q_b are the quantities of heat to heat the roller and the belt with the coal dust layer, respectively, W.

The friction coefficient μ of the roller–belt couple is higher when the friction system includes coal dust. As per State Standard GOST ISO 21182-2016, the modeling used $\mu = 2.0$ for the roller–belt system and $\mu = 3.4$ for the roller–coal dust–belt systems.

After evaluating the friction force at different input data, the heat quantity Q_{heat} generated in the off-normal mode of the conveyor is calculated.

Modeling stage II.

The process uniqueness conditions:

- Physical data of the roller material: steel, density $\rho_1 = 7850$ m³, heat conduction $\lambda_1 = 90$ W/(m·K), specific heat capacity $c_1 = 557$ J/(kg·K).

- Physical data of the belt material: density $\rho_2 = 1300$ m³, heat conduction $\lambda_2 = 10$ W/(m·K), specific heat capacity $c_2 = 971$ J/(kg·K).

- Initial condition: the ambient temperature t_a °C is equal to the roller and belt temperatures t_r and t_b °C.

The third-order boundary condition describes heat exchange between a body and the ambience [22, 23]:

$$Q_r = \alpha(t_r - t_0), \quad (4)$$

where α is the heat transfer coefficient; t_r and t_0 are the roller temperatures after the heat emission Q_r and at the initial time, respectively.

At the second stage of modeling in unit Transient Thermal, the roller experiences the heat Q_r . The heat flow on the roller is calculated from the formula:

$$Q_r = \alpha_{hf} Q_{heat}, \quad (5)$$

where α_{hf} is the heat flow pattern coefficient found from Sharron's [24].

Introducing actual values in the heat flow pattern formula:

$$\alpha_{hf} = \frac{\sqrt{\rho_1 \lambda_1 c_1}}{\sqrt{\rho_1 \lambda_1 c_1} + \sqrt{\rho_2 \lambda_2 c_2}}, \quad (6)$$

where ρ_1 is the roller steel density, kg/m³; λ_1 is the heat conduction of the roller material, W/(m·K); c_1 is the specific heat capacity of the roller material, J/(kg·K); ρ_2 is the density of the belt material, kg/m³; λ_2 is the heat conduction of the belt material, W/(m·K); c_2 is the specific heat capacity of the belt material, J/(kg·K); [25, 26], we obtain:

$$\alpha_{hf} = \frac{\sqrt{7850 \cdot 90 \cdot 557}}{\sqrt{1300 \cdot 10 \cdot 971} + \sqrt{7850 \cdot 90 \cdot 557}} = 0.85.$$

The roller material parameters for the thermodynamic modeling are: the absolute black's radiation constant $C_0 = 5.69$ W/(m²·deg⁴), the roller emissivity $\varepsilon = 0.95$, the heating rate $\alpha_1 = 6$ W/(m²·K) in natural convection.

Results and discussion

Modeling stage I.

The seizure modeling for the middle roller in the 4th row produced the values of the friction forces F_{fr} in the roller–belt and in the roller–coal dust–belt systems. The values were placed in formula (2) to find the heat quantity Q_{heat} .

The heat spent to heat the roller is found from (4) as:

$$Q_r = 0.85 Q_{heat}. \quad (7)$$

Tables 1 and 2 describe the heat in friction in the two test friction couples at the belt velocity $v = 2.15$ m/s and different belt pressures P (GOST 31558-2012).

Tables 3 and 4 describe the heat in friction in the two test friction couples at different belt velocities and at the belt pressure $P = 200$ N (GOST 31558-2012).

Modeling stage II.

Figure 1 illustrates the temperature pattern in the roller shell under the heat Q_{heat} .

The roller heating is nonuniform, and the highest temperature is observed at the contact with the belt.

Figure 2 shows the model temperature of the roller surface per fire stages [27, 28].

The minimal time up to the coal dust smolder under varied loading of the conveyor belt is 35 s (see Fig. 2a) and under varied velocity of the belt is 45 (see Fig. 2b). The time of the roller heating up to 100 °C, which conforms with fire phase 1.1, is 17 s (**Fig. 3**).

Figure 4 offers a graphical presentation of the heat balance equation for a roller: here, the roller heating Q_r is a sum of the heat absorbed by roller, Q_{rin} and the heat gone outward, Q_{rout} , including the convective heat Q_{con} and radiant heat Q_{rad} .

Initially, the energy of the heat flux is spent for the roller body heating, and the temperature of the roller surface grows fast in this period of time. The heat quantity gone outward increases with time, and the roller surface heating rate lowers gradually. When the outward-directed heat quantity approaches the value of the total heat directed to the roller and the roller-absorbed heat tends to zero, the temperature of the roller surface remains unaltered with time, and the energy is totally spent for the generation of the convective and radiant heat.

A fire-hazardous situation in the off-normal mode of a conveyor is described by heat balance equation (3) which sets that the friction-induced heat goes to warm the roller and the belt.

The heat Q_f mostly influences the roller according to equation (6). The belt passes the friction region too fast to get heated, and the heat Q_b has no material effect on the roller heating [29, 30].

The roller heat goes inside the roller to warm it – Q_{rin} and for generating the convective heat flux Q_{con} and radian heat flux Q_{rad}

$$Q_r = Q_{\text{rin}} + Q_{\text{con}} + Q_{\text{rad}} \quad (9)$$

The heat taken to warm the roller and the belt for the whole heating time T up to the temperatures t_r or t_b , respectively, is given by:

$$Q_{\text{rin}} = c_1 g_1 (t_r - t_0), \quad (10)$$

$$Q_{\text{bin}} = c_2 g_2 (t_b - t_0), \quad (11)$$

where g_1 and g_2 are, respectively, the masses of the roller and the belt, kg.

The convective heat flux:

$$Q_{\text{con}} = \alpha_1 S_p (t_1 - t_0), \quad (12)$$

where α_1 is the heat transfer coefficient of the roller material; S_p is the radiance area including the belt-uncovered areas and the end faces of the roller, m²; t_1 is the temperature in the heating zone, deg; t_0 is the ambient temperature, deg.

The radiance heat flux [16]:

$$Q_{\text{rad}} = \varepsilon C_0 S_p \left[\left(\frac{273 + t_1}{100} \right)^4 - \left(\frac{273 + t_0}{100} \right)^4 \right], \quad (13)$$

Table 1. Heat flow in roller–belt friction at belt velocity of 2.15 m/s

P, N	100	200	300	450	600	700	1000
F_{fr}, N	205.7	230.4	256.0	292.6	329.0	365.3	431.9
Q_{heat}, W	442.2	495.3	550.3	629.2	707.4	785.4	928.7
Q_r, W	375.9	421.0	467.8	534.8	601.0	644.6	789.4

Table 2. Heat flow in roller–coal dust–belt friction at belt velocity of 2.15 m/s

P, N	100	200	300	450	600	700	1000
F_{fr}, N	355.9	401.5	439.3	494.5	566.8	631.0	736.3
Q_{heat}, W	765.3	863.2	944.4	1081.6	1218.6	1356.6	1583.0
Q_r, W	650.5	733.7	802.7	919.4	1035.8	1153.1	1345.6

Table 3. Heat flow in roller–belt friction at belt pressure of 200 N

$v, m/s$	1.60	2.15	2.50	3.15
F_{fr}, N	226.60	230.40	235.70	235.00
Q_{heat}, W	362.50	495.30	589.30	740.00
Q_r, W	308.13	421.01	500.91	629.00

Table 4. Heat flow in roller–coal dust–belt friction at belt pressure of 200 N

$v, m/sc$	1.60	2.15	2.5	3.15
F_{fr}, N	400.30	401.50	404.6	406.30
Q_{heat}, W	640.50	863.20	1011.6	1279.70
Q_r, W	544.43	733.70	859.9	1087.70

where S_p is the radiance area including the belt-uncovered areas and the end faces of the roller, m²; C_0 is the absolute black's radiation constant, W/(m²·deg⁴); ε is the roller emissivity factor; t_1 is the temperature in the heating zone, deg; t_0 is the ambient temperature, deg.

If there is a layer of coal dust between the roller and the belt, some heat is spent for warming this layer.

The coal dust layer experiences simultaneously the heat from the conductance, radiance and convection, and from the heat spent for warming the belt:

$$Q_{\text{cd}} = Q_{\text{rin}}^* + Q_{\text{rad}}^* + Q_{\text{con}}^* + Q_b^*, \quad (14)$$

where Q_{cd} is the heat taken by coal dust, W; Q_{cond}^* , Q_{rad}^* , Q_{con}^* is, respectively, the heat from the conductance, radiance and convection, W; Q_b^* is the heat spent to warm the belt, W.

Participation of coal dust in friction increases the risk of fire as the rate of the temperature rise is lower in the friction system without coal dust at the same belt velocity and pressure.

The review of the belt fire detection systems [27] shows that the fastest fire detection is provided by the use of the distributed temperature fire-alarm box and the point gas fire-alarm box, which responds to the increased concentrations of CO. The ultra early fire detection requires that sensors and alarm boxes are arranged at the nearest distance from fire-hazardous sites.

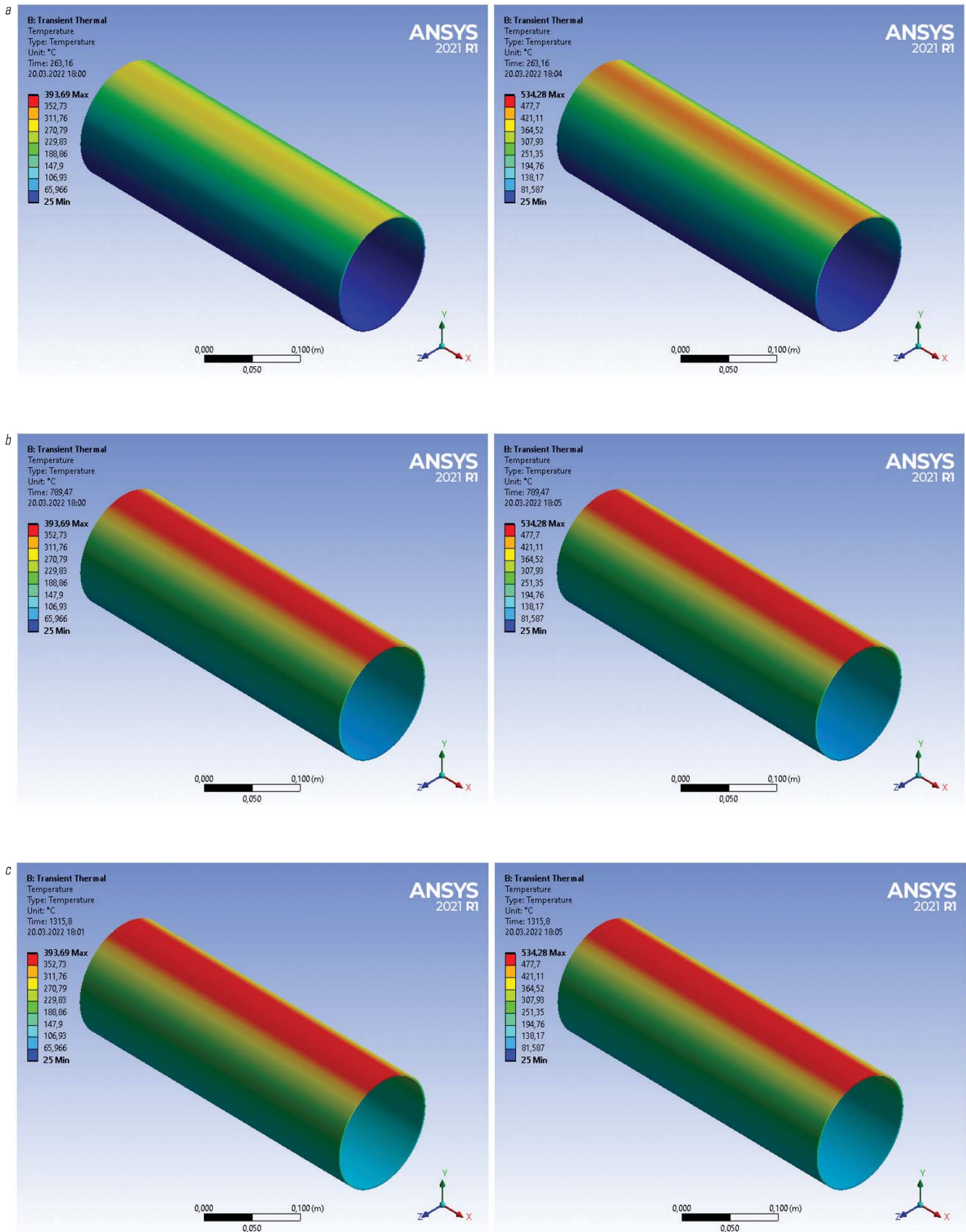


Fig. 1. Roller temperature after heating by Q_{heat} :
 $t = 263.16$ (a); $t = 789.47$ (b); $t = 1315.8$ (c)

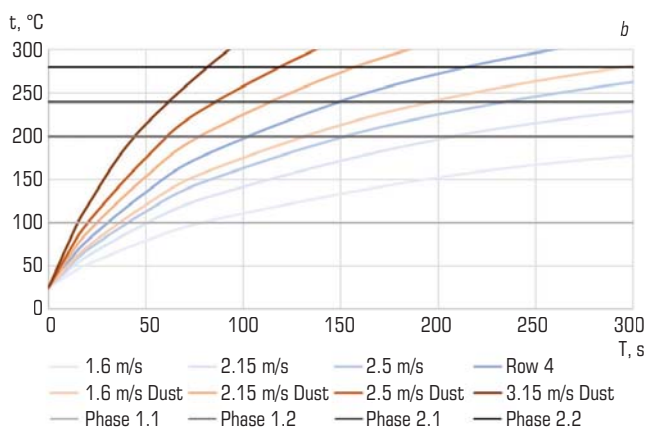
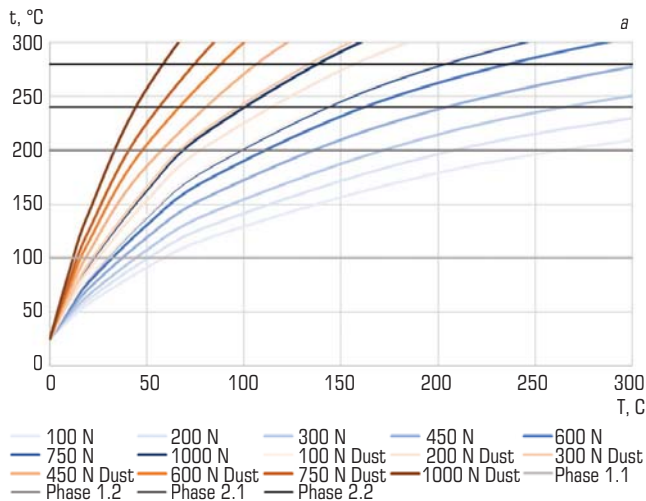


Fig. 2. Variation of surface temperature of roller at different values of pressure P (a) and belt velocity (b)

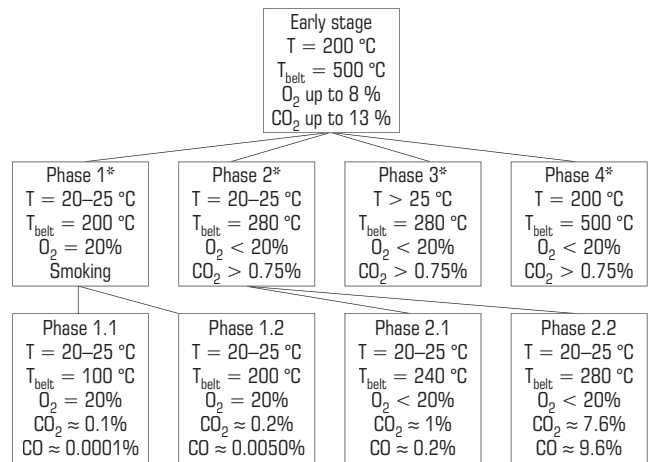
Conclusions

Heating of belt rollers due to friction on the loaded conveyor belt with and without coal dust has been modeled in ANSYS using the finite element method.

The modeling of fire initiation in the loaded belt and faulty roller friction has found that:

- the minimal time of fire detection at the ultra early stage of fire development is 17 s from the start of the off-normal mode operation of the conveyor;
- the coal dust participation in the belt—roller friction system increases the risk of fire;
- the heat affecting the roller divides into the absorbed heat, radiance heat and convection heat;
- the roller heat directed outward can cause inflammation of coal dust and other materials having the low inflammation temperature.

The total heat Q_{heat} generated in friction between the conveyor belt and the roller is described by the Amontons—Coulomb law using formula (2); heat balance equation (3) includes the roller heat Q_r and the belt heat Q_b . Coal dust in the belt—roller contact zone intakes some heat, which is absorbed and radiated by the roller, Q_{cd} gets dried and emits volatiles, CO and steam [31, 32]. When the pyrolysis temperature is



* Fire phases as per NIIGD classification (Donetsk) [3]

Fig. 3. Early-stage fire phases

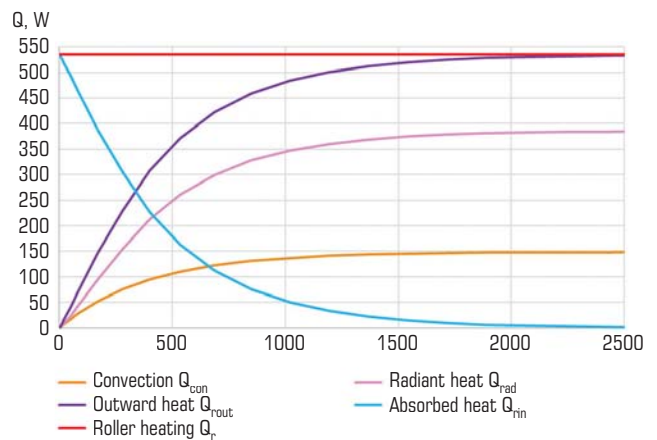


Fig. 4. Graphic presentation of heat conduction equation for friction-induced heating of belt conveyor roller

reached, which is different per coal grades, smoldering begins owing to the lack of oxygen in the combustion zone. In case of the continued heating of the roller surface that interacts with coal dust, flaming initiates and seizes all close-spaced elements in a longwall equipped with a belt conveyor [33, 34].

Improvement of the fire safety of belt conveyors requires an operation algorithm of engineering facilities capable to detect fire signs (CO concentration, high ambient temperature) [35] at the ultra early stage of fire development at the minimized false triggering. Precautions can include removal of coal dust layers from the load and return branches of conveyor belts.

References

1. Trufanova I. S., Serzhan S. L. Improving transportation efficiency belt conveyor with intermediate drive. *Journal of Mining Institute*. 2019. Vol. 237. pp. 331–335.

2. Yurchenko V. M. On the problem of fire safety of belt conveyors. *GIAB*. 2016. No. 2. pp. 134–144.
3. Azbel M. D. Multifunctional automated air and gas control in coal mines : Thesis of Dissertation of Doctor of Engineering Sciences. Kemerovo : FGUP Nauchnyi centr po bezopasnosti rabot v ugolnoy promyshlennosti, 2002. 42 p.
4. Grudachev A. Ya., Mishchenko T. P. Study of the support roller heating process in an emergency mode of belt conveyor operation. *Vestnik Donetsk National Technical University*. 2019. No. 1(15). pp. 26–31.
5. Barros-Daza M. J., Luxbacher K. D., Lattimer B. Y., Hodges J. L. Mine conveyor belt fire classification. *Journal of Fire Sciences*. 2021. Vol. 40, Iss. 1. pp. 44–69.
6. Chamorro J., Vallejo L., Maynard C., Guevara S., Solorio J. A. et al. Health monitoring of a conveyor belt system using machine vision and real-time sensor data. *CIRP Journal of Manufacturing Science and Technology*. 2021. Vol. 38. pp. 38–50.
7. Furukawa O. Fire detection of belt conveyor using random forest. *IEEE Transactions on Fundamentals and Materials*. 2021. Vol. 141, No. 9. pp. 508–513.
8. Lisakov S., Sidorenko A., Sypin E. Research on adaptation of multi-criterial electro-optical system under object in the form of belt roadway of coal mine for fire control. *XXII International Conference of Young Specialists on Micro/Nanotechnologies and Electron Devices*. 2021. pp. 287–295. DOI: 10.1109/EDMS2169.2021.9507631
9. Ray S. K., Khan A. M., Mohalik N. K., Mishra D., Varma N. K. et al. Methodology in early detection of conveyor belt fire in coal transportation. *Energy Sources, Part A: Recovery, Utilization and Environmental Effects*. 2020. pp. 1–19. DOI: 10.1080/15567036.2020.1823527
10. Shaportov A. V. Analysis of industrial safety and causes of fires on conveyor belts in ore and coal mines. *GIAB*. 2020. No. S1. pp. 57–65.
11. Saydulin E. G., Rukin M. V., Shelemba I. S., Vozhakov I. S., Cheverda V. V. Automatic detection of faulty conveyor belt rollers using TOREX fibre optic thermal sensor. *Gornaya promyshlennost*. 2020. No. 4. pp. 54–57.
12. Vyaltsev A. V., Frolov A. V. Probabilistic approach to estimation procedure of fire risk in friction in slip of drive drum of belt conveyor. *GIAB*. 2009. No. S12. pp. 125–128.
13. Hoff H. Using distributed fibre optic sensors for detecting fires and hot rollers on conveyor belts. *2nd International Conference for Fibre-Optic and Photonic Sensors for Industrial and Safety Applications (OFSIS)*. Australia : IEEE, 2017. pp. 70–76. DOI: 10.1109/OFSIS.2017.9
14. Litton C. D., Perera I. E. Evaluation of criteria for the detection of fires in underground conveyor belt haulageways. *Fire Safety Journal*. 2012. Vol. 51. pp. 110–119.
15. Danilov V. M., Erofeev A. V., Gorokhov T. I. Capabilities of software package ANSYS in solution of basic and applied problems in construction. *Molodye uchenye—razvitiyu Natsionalnoi tekhnologicheskoi initsiativy (POISK)*. 2021. No. 1. pp. 182–185.
16. Mersha T. K., Du C. Co-simulation and modeling of PMSM based on ANSYS software and SIMULINK for EVs. *World Electric Vehicle Journal*. 2022. Vol. 13, Iss. 1. DOI 10.3390/wevj13010004
17. Korneev S. V., Dolgikh V. P. Structuring of computer model of load—conveyor belt—rollers in software ANSYS Workbench. *Collection of Research Papers of the National Mining University*. 2014. Vol. 45. pp. 105–111.
18. Breki A. D., Chulkin S. G., Gvozdev A. E., Kolmakov A. G. A generalized mathematical model of external sliding friction in solids. *Inorganic Materials: Applied Research*. 2022. No. 13. pp. 967–971. DOI:10.1134/S2075113322040062
19. Taylor R. I. Rough surface contact modelling : A review. *Lubricants*. 2022. Vol. 10, Iss. 5. DOI 10.3390/lubricants10050098
20. Mikhailenko S. A., Sheremet M. A. Convection in a differentially heated cubic cavity rolling about horizontal axis. *International Journal of Thermal Sciences*. 2022. Vol. 179. pp. 3–15. DOI:10.1016/j.ijthermalsci.2022.107639
21. Richter C., Fessel K., Katterfeld A., Chumachenko Y. Application scenario of the internet of things at the example of overheated roller in belt conveyors. *Logistics Journal*. 2019. DOI:10.2195/lj_Proc_richter_de_201912_01
22. Jaber S. B., Hamilton A., Xu Y., Kartal M. E., Gadegaard N. et al. Friction of flat and micropatterned interfaces with nanoscale roughness. *Tribology International*. 2021. Vol. 153. DOI:10.1016/j.triboint.2020.106563
23. Izmailov V. V., Novoselova M. V. Influence of temperature and temperature prehistory on frictional characteristics of metal friction pairs. *Journal of Friction and Wear*. 2021. Vol. 41. pp. 497–501.
24. Amosov A. P. Elemental thermal models of friction. *Izvestiya Samarskogo nauchnogo tsentra Rossiyskoi akademii nauk*. 2011. Vol. 13, No. 4-3. pp. 656–662.
25. Xiao Y., Chen L., Zhang X., Ren, S., Li D. Controlling fire of belt conveyor and ventilation network calculation in underground coal mines. *Conference Series: Earth and Environmental Science*. 2018. No. 189. DOI:10.1088/1755-1315/189/4/042028
26. Tolkahev O., Klychko A., Dickenstein I. The heat exchange of the drive drum and full slipped conveyor belt. *Vestnik Instituta grazhdanskoy zaschity Donbassa*. 2015. No. 1. pp. 62–66.
27. Shaportov A. V. Fire protection systems on conveyor transport in mines. *GIAB*. 2022. No. 7. pp. 68–78.
28. Artamonov V. S., Polyakov A. S., Ivanov A. N. Ultraearly and early fire detection: terms, limits of use and unity. *Fire and Explosion Safety*. 2016. Vol. 25, No. 9. pp. 78–83.
29. Mansurov R. Sh., Voskoboinikov Yu. E., Boeva V. A. Heat transient processes identification of the elements of internal environment system. *Vestnik MGSU*. 2022. Vol. 17, No 2. pp. 222–231.
30. Shaimerdenova K. M., Schragger E. R., Tussybaeva A. S., Nausharban Zh. K. Investigation of heat exchange processes in vertically arranged heat exchangers. *Bulletin of the Karaganda University. Physics Series*. 2019. No. 2(94). pp. 66–72.
31. Novoselov S. V., Popov V. B., Golik A. S. Risk assessment of endogenous fires in coal mines. *Ugol*. 2020. No. 5(1130). pp. 21–25.
32. Igishev V. G., Shlapakov P. A., Haimin S. A., Sin S. A. Fire indicator gases liberation at coal oxidation at the stage of self-heating and flameless combustion. *Bulletin of Research Center for Safety in Coal Industry (Industrial Safety)*. 2015. No. 4. pp. 55–59.
33. Ushanova S. E., Ziborova E. Yu. Increasing the durability of friction units for mining equipment and conveyor transport. *GIAB*. 2020. No. S5. pp. 3–8.
34. Dmitrieva V. V., Sizin P. E. Reliability evaluation of belt conveyor line at different redundancies of carrying rollers. *GIAB*. 2021. No. 7. pp. 85–95.
35. Balovtsev S. V., Vorobyeva O. V. Multifunctional systems of industrial safety in coal mining industry. *GIAB*. 2020. No. S1. pp. 31–38. **EM**